

## Supplementary material

We also used a Langmuir trough NIMA 602 BAM (NIMA, UK) to measure the surface tension  $\gamma$  versus area  $A$  isotherms for the mixed surfactant-particle layers adsorbed at the dispersion surface.

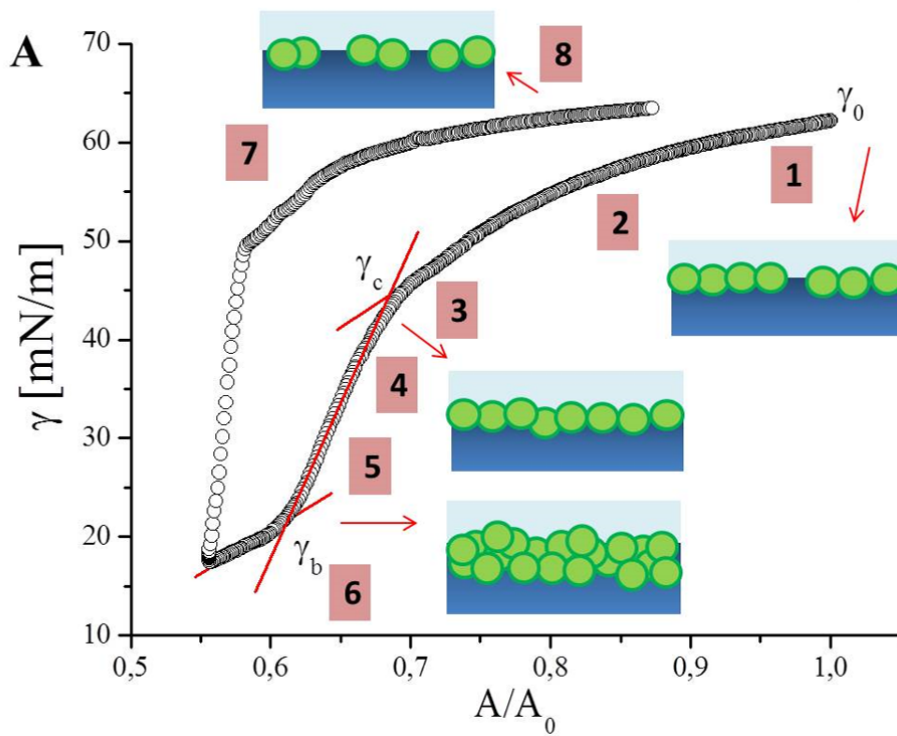
### 1. Methods

The compression/expansion cycles were started once  $\gamma_0$  was reached and performed at the slowest available speed of 5cm<sup>2</sup>/min. We used a Wilhelmy plate (Whatman CHR1 chromatography paper) parallel to the barriers to measure the surface pressure. The Langmuir trough is coupled to a Brewster angle microscope (Nanofilm, Germany) in order to image the interface during the compression/expansion cycles at an angle of incidence of 53° (Brewster's condition at the air/water surface, for which pure water shows no visible reflection). This allows detecting the presence of ultrathin surface layers. The images were recorded using a CCD camera (60 Hz), with a lateral resolution below 20  $\mu$ m. The field of view is 4.8  $\times$  6.4 mm<sup>2</sup>.

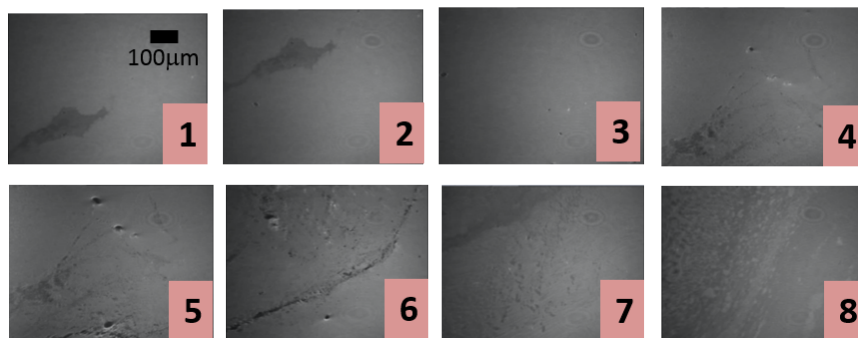
### 2. Observations

Figure S1A shows the compression expansion cycle for a sample containing 10<sup>-4</sup> M of CTAB and 1wt% of SiO<sub>2</sub> particles. After equilibration (constant surface tension  $\gamma_0=60$ mN/m), the surface is compressed at constant speed ( $dA/dt=5$ cm<sup>2</sup>/min). The decrease of  $\gamma$  is shown Figure S1A, where the area of the layer  $A$  is normalised by the initial area  $A_0$ . The sequence of BAM images in Figure S1B shows the evolution of the surface layer upon compression. Different regimes can be observed during the compression and expansion cycles:

(i) *Initial compression of the adsorbed monolayer.* In this region  $\gamma$  decreases smoothly from  $\gamma_0$  with the area. Images 1 and 2 correspond to the morphology observed in this regime, where a thick layer of particles coexists with thin regions of free surfactant, not complexed with particles. In all the cases studied, the proportion of thin regions is small compared to the thick ones but the thin regions move freely, so the surface layer is fluid in this regime. The coexistence of thin and thick surface regions could be related to the existence of capillary attractive forces between particles that tend to form dense surface clusters.<sup>1</sup>



**B**



**Fig. S1: BAM and Compression in a Langmuir trough.** (A) Surface tension as a function of the normalised surface area  $A/A_0$ . The cartoons show the hypothesised lateral view of the interface covered by surfactant-decorated particles in the different regimes. (B) BAM images corresponding to the regions from 1 to 8 in the  $\gamma$ - $A$  isotherm.

(ii) Jamming transition (at  $\gamma=\gamma_c$ ). When  $\gamma$  reaches the value  $\gamma_c$ , one observes the disappearance of the thin regions (image 3). Upon compression of the layer the thick domains merge, yielding a homogenous layer. Upon further compression, one observes regions with different textures (image 4), separated by defects –possibly dislocations– which suggest that the surface layer is solid-like and that the transition at  $\gamma_c$  is a jamming transition.

(iii) Jammed state ( $\gamma < \gamma_c$ ). Figure A1 shows that the slope of the  $\gamma$ - $A$  isotherm, which is related to the compressional elastic modulus  $E(=d\gamma/d\ln A)$  is larger than in the fluid region. Interestingly it is also constant during compression, with a rather high value of around 130 mN/m. This is much higher than measured using the bubble compression due to the shear component that also contributes in the Langmuir trough. This change of slope is clearly associated with the fluid to solid transition observed. Further compression exerted by the barriers leads to an evolution of the morphology of the surface, which becomes less homogeneous, the amount of defects increasing as the compression continues (image 5).

(iv) Buckling transition ( $\gamma = \gamma_b$ ). A buckling transition is reached at  $\gamma = \gamma_b = 22.5 \pm 0.5$  mN/m. Image 6 shows the existence of out-of-plane distortions at random positions, the entire planar interface becoming crumpled. The compression surface stress is too large for the layer to respond with in-plane deformations. It is noteworthy that the morphologies observed are stable over a period of at least several hours.

(v) Expansion cycle: existence of hysteresis. Once the buckled state has been reached, we started an expansion of the surface by opening the barriers of the trough. The solid layer then breaks into separate domains (images 7 and 8) which remain stable over several hours. The surface tension increases suddenly as a consequence of the expansion. An important hysteresis is seen in the  $\gamma$ -A isotherm. The layer texture is somewhat different in the expansion cycle (images 7 and 8) than in the compression cycle, and with different surface packing densities, explaining why the final surface tension is slightly different from  $\gamma_0$ .

This behavior is very similar to the one seen for adsorbed layers of partially hydrophobic particles with the difference that the surface tension varies before the particle domains come into contact as in the presence of free surfactant.<sup>2</sup> Similar results were also reported for latex particles at oil-water interfaces.<sup>3</sup> In all these cases, the surface tension does not vanish as it should at the onset of the buckling transition. This could be because below  $\gamma_b$ , the surface layer is solid, and that the measured surface tension is an apparent tension and contains contributions from the shear elastic moduli.<sup>2</sup> Or because the methods to measure surface tension might not be very meaningful after buckling is reached.

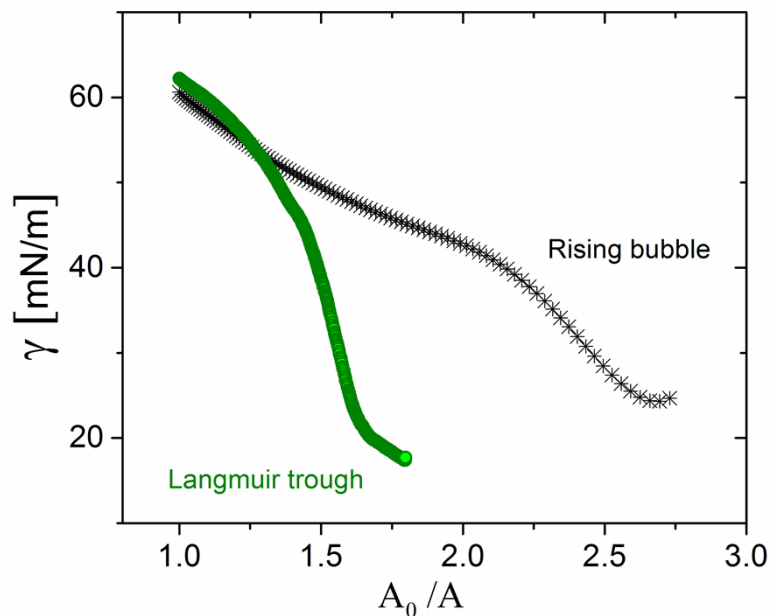


**Fig. S2: Comparison between planar and curved geometries:** Surface tension versus normalized Area of a Sample with  $10^{-4}$ M CTAB performed in a Langmuir trough and in a rising tensiometer.

### 3. Comparison with the bubble compression

The compression experiment has been performed both on individual bubbles and on a Langmuir through. The results are compared in Figure S2 for a solution containing  $10^{-4}$  M of CTAB. The values observed for  $\gamma_b$  and  $\gamma_c$  are similar but the whole curve is quite different. The nature of the deformations is very different in the two experiments. While the compression of a bubble leads to a nearly isotropic compression within the surface, the uni-axial compression in the Langmuir trough combines isotropic compression with shear.<sup>2,4</sup> The importance of the shear contributions increases with solidification of the layer, which is exactly what is observed in Fig. S2: while the surface tension curves are quite similar at low surface coverage they diverge for higher surface coverage. The presence of the shear contribution in the Langmuir trough should lead to a higher elastic modulus than in the case of the bubble, which is what is

observed. There are surely also kinetic effects due to the difference in compression velocities (more than 100 times faster with the bubbles). Last but not least, evaporation effects in the Langmuir trough may lead to a different organization of the particles at the interface.

1. M. Oettel, S. Dietrich, *Langmuir*, 2008, **24**(4), 1425-1441.
2. D. Y. Zang, E. Rio, D. Langevin, B. Wei, B. P. Binks, *European Physical Journal E*, 2010, **31**(2), 125-134.
3. C. Monteux, J. Kirkwood, H. Xu, E. Jung, G. G. Fuller, *Physical Chemistry Chemical Physics*, 2007, **9**(48), 6344-6350
4. A. Yeung, L. C. Zhang, L. C. *Langmuir*, 2006, **22**,(2), 693-701.